Journal of Alloys and Compounds 509 (2011) 6683–6688

Contents lists available at ScienceDirect

Journal of Alloys and Compounds

journal homepage: www.elsevier.com/locate/jallcom

A novel technique for production of nano-crystalline mono tungsten carbide single phase via mechanical alloying

Mansour Razavi*, Mohammad Reza Rahimipour, Rahim Yazdani-Rad

Materials and Energy Research Center (MERC), P.O. Box 14155-4777, Tehran, Iran

ARTICLE INFO

Article history:
Received 3 January 2011
Received in revised form 20 March 2011
Accepted 23 March 2011
Available online 1 April 2011

Keywords:
Mono tungsten carbide
Mechanical alloying
Nano-crystalline

ABSTRACT

Due to simultaneous synthesis of WC and W_2C phases in most of the synthesis processes and lower mechanical properties of W_2C than WC, in this work the possibility of production of nano-crystalline WC single phase as a useful refractory ceramic by means of mechanical alloying has been investigated. The raw materials containing W and C with WC were milled in a planetary ball mill. The sampling has been done in different times. As it was expected, XRD studies showed that after 75 h of milling the WC with W_2C were produced. By adding WC to the raw materials in the beginning of the process it led to the fact that after 50 h of milling WC was synthesized only without any other phases which remained stable at the higher times while milling. During broadening of XRD peaks, the size of synthesized crystalline WC was estimated in the order of nano-meter. Crystalline size and mean strain of synthesized WC in the system without additive were higher and lower than the system containing WC, respectively.

1. Introduction

Usage of WC has spread in cutting and wear resistance industries due to high hardness (2600 HV), good toughness, high melting point (2780 °C), high wear resistance, suitable resistance in thermal shock and good thermal conductivity. Its natural resistance to oxidation and corrosion of this material at high temperature cause the increase usage of this material as coating in high temperature [1–6].

Direct reaction of W and C in high temperature (1400–1600 °C) under vacuum or inert gas with high purity is know as the conventional method for production of this material, but this process is costly [2,7]. Instead of pure W, tungsten oxide can be used with a strong reducing agent such as magnesium [8]. In addition fluid bed, self-propagating techniques, organometallic precursor, solution state and electro chemical methods have been used for production of this carbide, but each of these methods have their specific advantages and disadvantages [9]. Due to limitations for synthesizing this material by traditional methods and considering the fact that the range of WC in the phase diagram is narrow, mechanical alloying can be a suitable method for production of nano-structured WC [10]. High-energy ball milling processes are commonly known as MM single component or mechanical alloying. High-energy ball milling can induce microstructural modifications and produce various non-equilibrium materials such as supersaturated solid solutions, amorphous alloys, nano-crystalline materials and so on [11].

Usually during the production process of tungsten carbide, WC and W_2C are synthesized together. Also the existence of other phases such as $W_6C_{2.54}$ and WC_{1-x} is possible. Because of W_2C is more brittle than WC, presence of W_2C with WC can be reduced tribology properties of final materials [2,10,12–17]. According to this phenomenon, the production of WC single phase in nano-meter scale via mechanical alloying has been tried in this paper.

2. Experimental

In this research, three raw materials were used: W with purity of 99.5% and mean particle size of 1 μm, amorphous carbon with purity of 99% and mean particle size of 0.5 μm black as carbon source and WC with purity of 99% and mean particle size of 1 μm.

These materials were milled by stoichiometric ratio (W + C = WC) in a planetary ball mill. The sampling has been carried out in different times (1, 2, 5, 10, 15, 20, 30, 50, 75, 100, 125 and 150 h). In order to protect materials from oxidation and undesirable reaction, the argon gas with purity of 99.99% and pressure of 250 kPa was utilized in cup of ball mill. The velocity of disk and cup of ball mill was 410 and 700 rpm, respectively. The used cup and balls were made from high chrome stainless steel. The ratio of balls to powder was 10:1 and from 4, 3 and 3 balls of 21, 16 and 10 mm, respectively which were used in all tests.

For determination of synthesized components as well as calculation of crystalline size (Williamson–Hall and Scherrer methods) [18,19], XRD instrument (Siemens model) with voltage and current of 25 mA and 30 kV, respectively and Cu Kα (λ = 1.5405 Å) radiation was employed.

In order to determination the full-width at half-maximum (FWHM), PANalytical X'Pert HighScore software was used. X'Pert HighScore uses the Pseudo-Voigt profile

* Corresponding author. Tel.: +98 261 6204131; fax: +98 261 6201888.
E-mail addresses: m-razavi@merc.ac.ir, m7816006@yahoo.com (M. Razavi).

0925-8388/$ – see front matter © 2011 Elsevier B.V. All rights reserved.
doi:10.1016/j.jallcom.2011.03.137

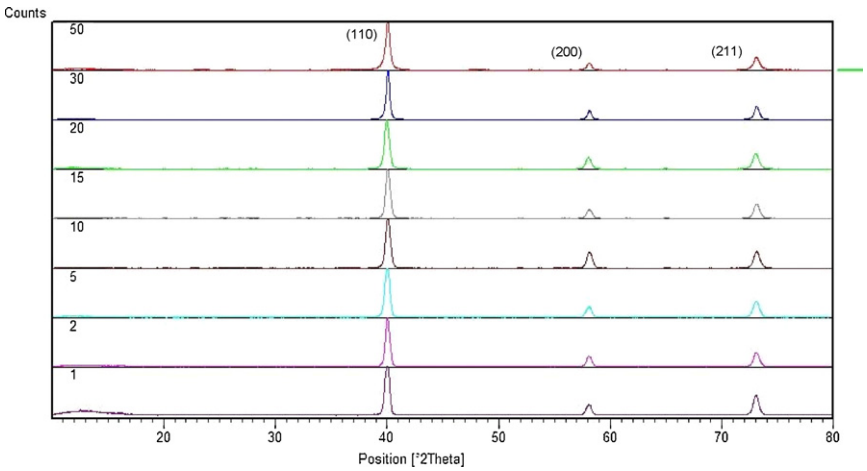

Fig. 1. X-ray patterns of samples containing W and C, which were milled from 1 to 50 h.

function, which is the weighted mean between Lorentz and Gauss function:

$$G_{ik} = \gamma \frac{C_0^{1/2}}{H_k \pi} [1 + C_0 X_{ik}^2]^{-1} + (1-\gamma) \frac{C_1^{1/2}}{H_k \pi^{1/2}} \exp[-C_1 X_{ik}^2]$$

where $C_0 = 4$, $C_1 = 4 \times \ln 2$, H_k is FWHM of the kth Bragg reflection, $X_{ik} = (2_{\theta i} - 2_{\theta k})/H_k$. γ is a refinable mixing parameter describing the amount of Gaussian profile versus the amount of Lorentzian profile; thus describing the overall profile shape. Also for removing of instrument broadening, pure WC which was annealed at 800 °C for 5 h under argon gas has been used as a standard sample.

3. Results and discussion

3.1. W–C system

X-ray patterns of samples containing W and C, which were milled to 50 h, are presented in Fig. 1. As seen in this figure, milling did not affect the type of phases, and in all milling times the W was the only phase which appears in patterns. As noted before, since the carbon source was selected in amorphous form, the C peaks cannot be seen in the diffraction pattern. However, even if the carbon was not amorphous, due to egregious difference between the mass absorption coefficients of the two materials, the chance of detecting the C peaks has been very weak ($MAC_W = 172.07\ cm^2/g$ and $MAC_C = 4.30\ cm^2/g$). By increasing the milling time, the peaks were broadened slightly, i.e. the crystalline size has been reduced by increasing the time. Another important fact in Fig. 1 was the reduction of area under peak 1 0 0 of W (1 0 0) that illustrates the gradual consumption of raw materials (Fig. 2) [19]. By increasing the milling time to 75 h, the peaks containing WC, W_2C and W were appeared (Fig. 3). In the milling time of 100 h, W peaks were disappeared completely while the WC peaks phase appeared much stronger. From xpowder software (version 2004.04.45 pro.) the ratio of visible materials in X-ray diffraction patterns in Figs. 1 and 3 have been calculated. These information are listed in Table 1. From this table, it is obvious that by increasing the milling time, the ratio

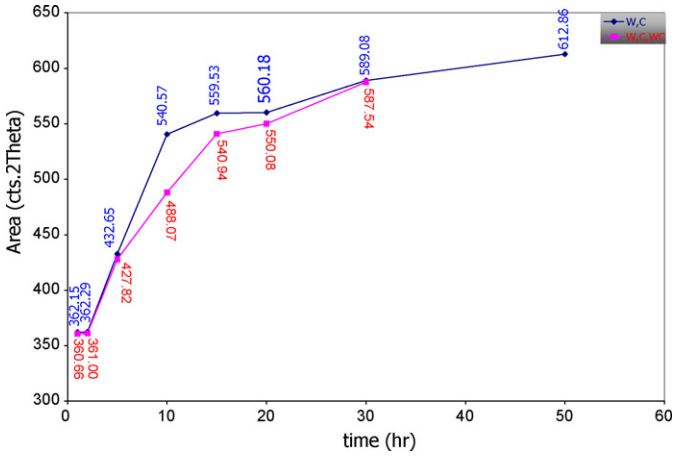

Fig. 2. The change of area of under peak 1 0 0 of W vs. milling time in system with primary WC and without any additives.

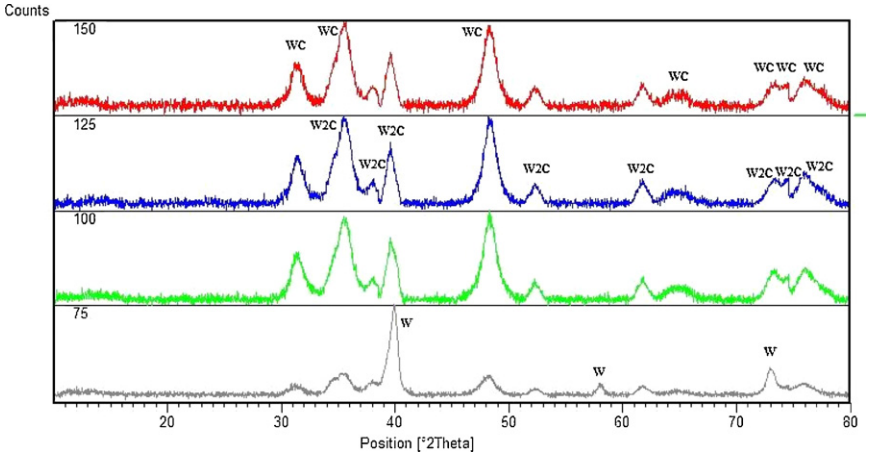

Fig. 3. X-ray patterns of samples containing W and C, which were milled from 75 to 150 h.

Table 1
The ratio of visible material in X-ray diffraction pattern.

		Milling time (h)											
		1	2	5	10	15	20	30	50	75	100	125	150
W–C system	W	1.000	1.000	1.000	1.000	1.000	1.000	1.000	1.000	0.228	–	–	–
	WC	–	–	–	–	–	–	–	–	0.161	0.549	0.553	0.581
	W_2C	–	–	–	–	–	–	–	–	0.611	0.451	0.447	0.419
W–C–WC system	W	1.000	1.000	1.000	1.000	1.000	1.000	1.000	0.936	0.544	–	–	–
	WC	–	–	–	–	–	–	–	0.064	0.456	1.000	1.000	1.000
W–C–Al_2O_3 system	WC	–	–	–	–	–	–	–	–	–	–	–	0.785
	W_2C	–	–	–	–	–	–	–	–	–	–	–	0.215

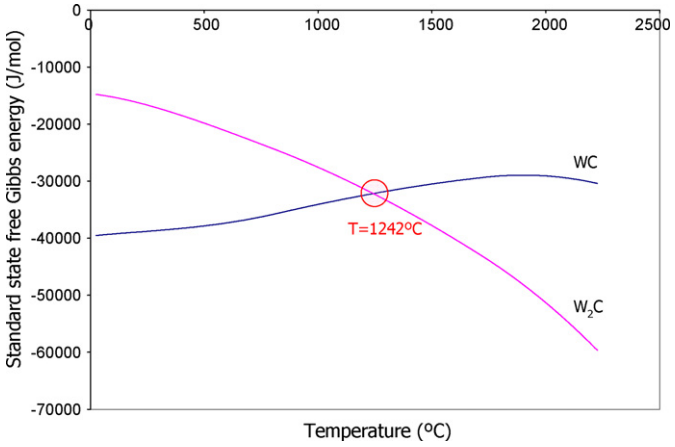

Fig. 4. Elingham–Richardson diagram of WC and W_2C phases.

of WC to W_2C was increased, however, even at 150 h the W_2C phase has not been eliminated from synthesized materials.

From the thermodynamic viewpoint stability of WC and W_2C phases at each temperature are expected regarding the Elingham–Richardson diagram (Fig. 4). Also the amounts of standard Gibbs free energy of reactions are illustrated in Table 2. On the basis of Fig. 4 and Table 2, W_2C is stable at temperature over 1242 °C and below this point WC is stable instead. From information of Table 2 and heat capacity of tungsten carbide, adiabatic temperature of reaction between W and C in room temperature can be calculated [20]. This value is about 900 °C, which is lower than the equilibrium temperature between WC and W_2C phases; hence in this temperature WC is stable phase. Since mechanical alloying is well known process for its capability of forming metastable or even non-equilibrium phases, W_2C as a metastable phase was formed and remained stable in the final products in this process [21].

3.2. W–C–WC system

In order to remove the undesirable W_2C phase from the synthesized materials, 1 wt.% of WC with stoichiometric ratio of W and C has been charged with the raw materials in the cup of ball mill. The results of XRD patterns from the milled materials up to 30 h are illustrated in Fig. 5. Similar to the previous system, by increasing the time of milling slight broadening of the peaks occurred and the area under peak 1 0 0 (Fig. 2) was decreased. Also as it can be seen in Fig. 2, the area under peak 1 0 0 in the sample containing 1 wt.% WC is smaller than that of the one without primary WC. Since the mass adsorption coefficient of WC is smaller than W ($MAC_{WC} = 161.78\ cm^2/g$), hence, as it was expected, the intensity of peaks and therefore area under the peaks of specimen containing WC were smaller than first system. Moreover, as it can been seen from Fig. 6, milling up to 50 h could caused the synthesizing of mono WC partially with primary W. Thus, by increasing the milling time, W phase gradually diminished while the amount of WC was increased. At 100 h the peaks of W was disappeared completely and the only visible peak belongs to WC. The WC phase until 150 h remained stable and did not show any changes. Quantities of phases in final composition according to X-ray pattern and the mentioned software are listed in Table 1. In this system, with reducing the synthesis time of WC, mono WC was produced which can be attributed to the following phenomena:

1. Formation of WC from W and C can be divided into three stages: first nucleation, second growth of these nucleation (grain growth) and finally in the third stage grains reach towards each other and thus, stop their growth. In the system containing WC, all or part of the first mentioned stage has been happening, so the transition time of raw materials to products should have been reduced. In other words, seeding of WC provides nuclei for the growth of WC and thus overcomes the nucleation barrier, which greatly enhances the formation of WC. As a result, single-phase WC was formed [22].
2. Presence of the ceramic phase accelerates the rate at which the milling process reaches completion. Therefore, the presence of WC particles increases local deformation, which improves the particle welding process. Beside this, the higher local deformation imposed by reinforcement particles increases the deformation hardening, which itself helps the fracture phe-

Table 2
The amount of standard state Gibbs free energy of formation of WC and W_2C.

Reaction	$\Delta G\ (J/mol) = a + b{\cdot}T + c{\cdot}T{\cdot}\ln T + d{\cdot}T^2 + e/T$					Temperature (K)	
	a	b	c	d	e	Min	Max
W + C = WC	−47390.769531	128.772995	−19.599999	0.017190	369000	298	1000
	−43972.765625	89.875054	−13.870000	0.013685	−227500	1000	1100
	−37796.898438	−63.644211	10.450001	−0.005565	−1721500	1100	2000
	88063.609375	−797.220886	107.440003	−0.033430	−45062000	2000	2500
W + ½C = ½ W_2C	−41466.800781	268.506744	−42.279999	0.018090	607000	298	1000
	−34630.800781	190.710876	−30.820000	0.011080	−586000	1000	1100
	−28454.933594	37.191650	−6.500000	−0.008170	−2080000	1100	2000
	223266.093750	−1429.961670	187.480011	−0.063900	−88761000	2000	2500

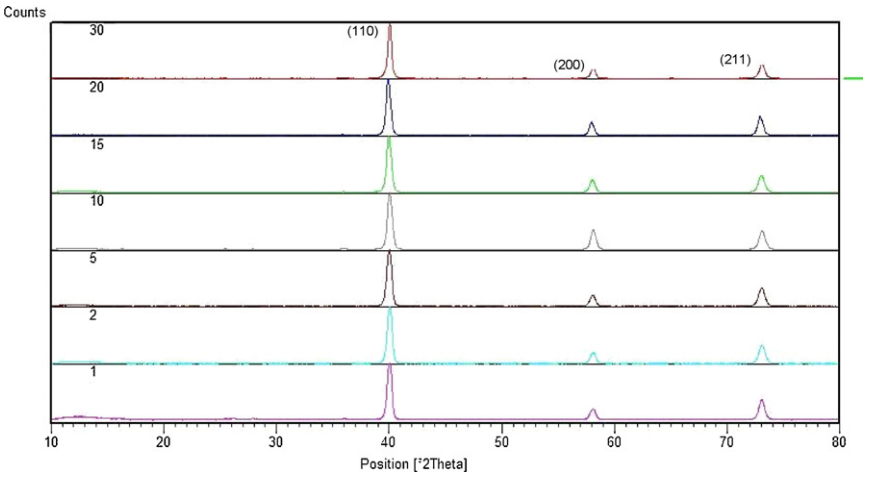

Fig. 5. X-ray patterns of samples containing W, C and WC, which were milled from 1 to 30 h.

nomenon. The small hard brittle particles in the matrix act as small milling agents, which lead to reduce the steady state milling time [23]. If this hypothesis was correct, then this treatment should occur by adding of other additives. In order to verify this, 1 wt.% α-alumina was added to mixture of W and C and these materials milled to 150 h with the former experimental conditions. X-ray diffraction pattern of this mixture and amount of produced phases are shown in Fig. 7 and Table 1, respectively. Despite the formation of W2C in the final composition, the amount of this phase in present system was much less than the system without any additive, which confirms the mentioned hypothesis.

3.3. Investigation of crystalline size and mean strain

In Fig. 8a, Williamson–Hall curve for determination of crystalline size and mean strain of synthesized WC phase is shown. The results of these calculations are listed in Table 3. As it can be seen in Table 3 and Fig. 8b, synthesized carbide had nano-meter scale (8–69 nm) where by increasing the milling time, the crystalline size is reduced and mean strain increased. Furthermore, the crystalline size of system containing WC and Al_2O_3 was smaller than the system without additive while the mean strain in these systems was higher than the first system, which can be confirmed the second hypothesis.

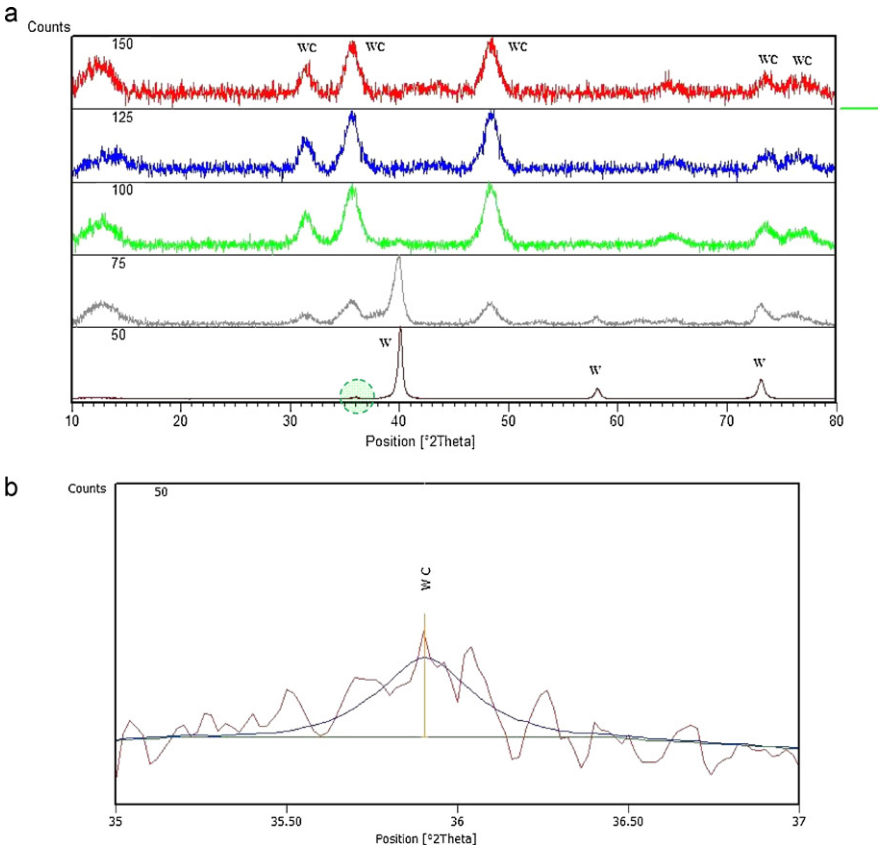

Fig. 6. X-ray patterns of (a) samples containing W, C and WC, which were milled from 50 to 150 h, (b) zoomed and fitted curve of the highlighted area of the XRD pattern above.

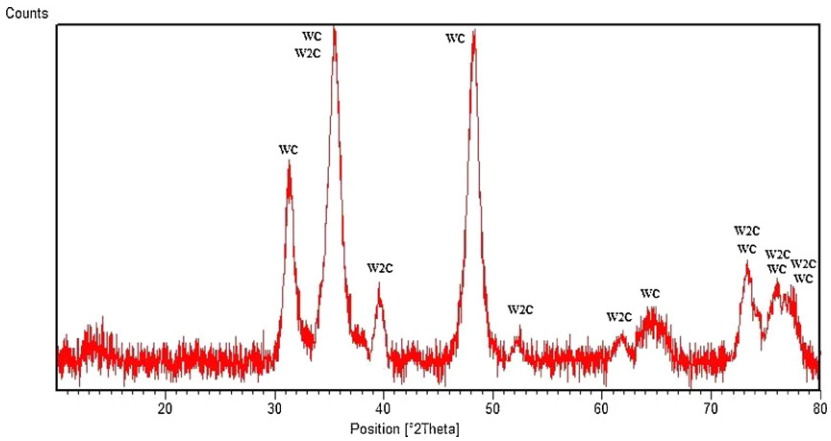

Fig. 7. X-ray patterns of samples containing 1 wt.% α-alumina.

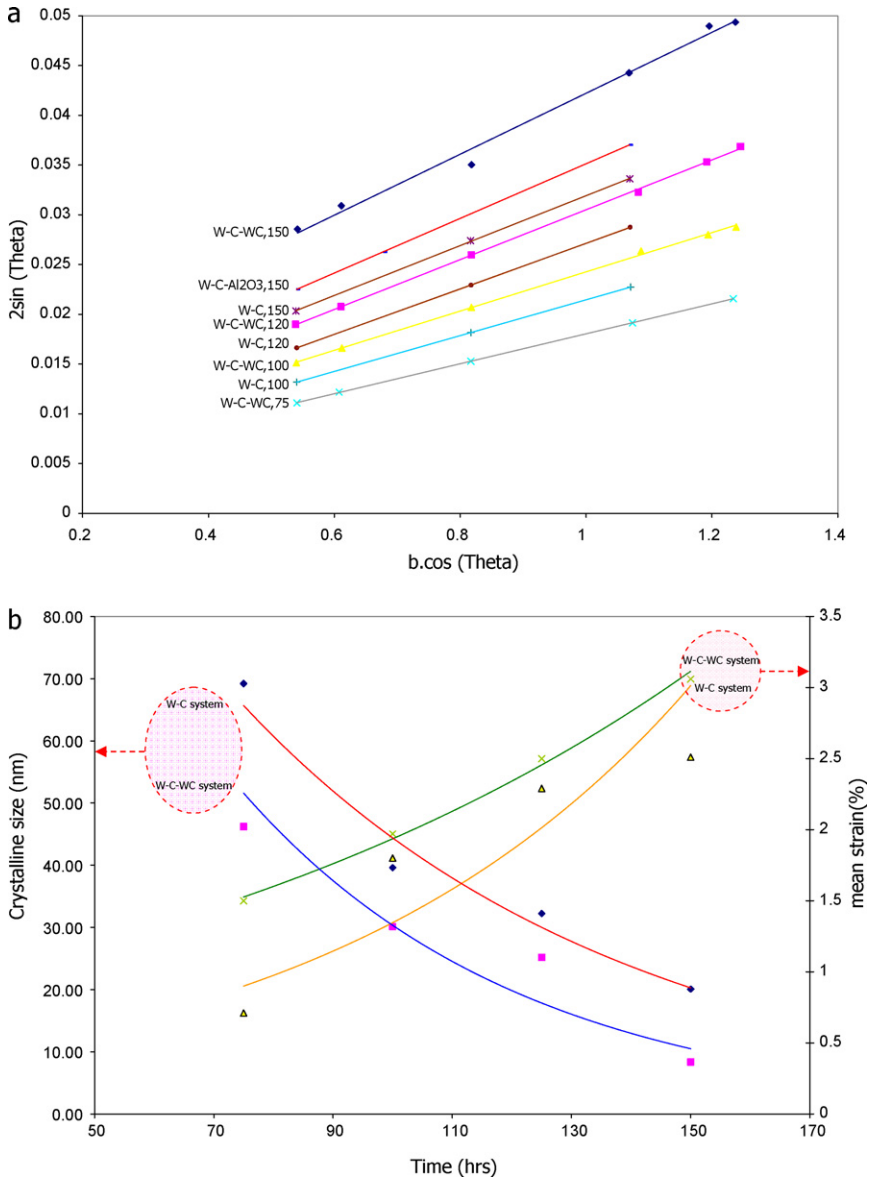

Fig. 8. (a) Williamson–Hall curve for determination crystalline size and mean strain of synthesized WC phase, (b) the change of crystalline size and mean strain of WC vs. milling time.

Table 3
Crystalline size and mean strain of synthesized WC.

	Time (h)	$y = ax + b$		Crystalline size (nm)	Mean strain (%)	Determination method
		a	b			
W–C system	75	–	–	69.21	0.71	Scherrer
	100	0.018	0.004	39.60	1.80	W–H
	125	0.023	0.004	32.23	2.29	W–H
	150	0.025	0.007	20.09	2.51	W–H
W–C–WC system	75	0.015	0.003	46.20	1.50	W–H
	100	0.020	0.005	30.13	1.97	W–H
	125	0.025	0.006	25.20	2.50	W–H
	150	0.031	0.017	8.35	3.06	W–H
W–C–Al_2O_3 system	150	0.026	0.008	18.00	2.57	W–H

4. Conclusion

By adding WC to the mixture of W and carbon black unlike the system without any additive, mono WC single phase was synthesized. Furthermore, the synthesis time has been reduced significantly. Adding WC can act as small balls, which helps in milling process. Also the existence of primary WC nucleus could be another reason for this phenomenon. By increasing the time of milling, the crystalline of synthesized carbide were fine and became the scale of nano-meter (8–69 nm) and the mean strain of the system was increased. The crystalline size and mean strain of the system containing WC were lower and higher than the system without additive, respectively.

References

[1] I.J. Shon, B.R. Kim, J.M. Doh, J.K. Yoon, K.D. Woo, J. Alloys Compd. 489 (2010) L4–L8.
[2] R. Yang, T. Xing, R. Xu, M. Li, Int. J. Refract. Met. Hard Mater. 29 (2011) 138–140.
[3] X.Q. Li, H.W. Xin, K. Hu, Y.Y. Li, Trans. Nonferrous Met. Soc. China 20 (2010) 443–449.
[4] M. Sakaki, M.S. Bafghi, J. Vahdati Khaki, Q. Zhang, F. Saito, J. Alloys Compd. 486 (2009) 486–491.
[5] Y. Shinoda, T. Akatsu, F. Wakai, Mater. Sci. Eng. B: Adv. 148 (2008) 145–148.
[6] T. Ryu, M. Olivas-Martinez, H.Y. Sohn, Z. Fang, T.A. Ring, Chem. Eng. Sci. 65 (2010) 1773–1780.
[7] K.M. Tsai, C.Y. Hsieh, H.H. Lu, Ceram. Int. 36 (2010) 689–692.
[8] C. Wu, S. Zhu, J. Ma, M. Zhang, J. Alloys Compd. 478 (2009) 615–619.
[9] J.H. Ma, Y.H. Du, J. Alloys Compd. 448 (2008) 215–218.
[10] Y. Jin, D. Liu, X. Li, R. Yang, Int. J. Refract. Met. Hard Mater. 29 (2011) 372–375.
[11] M. Razavi, M.R. Rahimipour, R. Mansoori, J. Alloys Compd. 450 (2008) 463–467.
[12] S. Bolokang, C. Banganayi, M. Phasha, Int. J. Refract. Met. Hard Mater. 28 (2010) 211–216.
[13] M. Zakeri, M.R. Rahimipour, S.K. Sadrnezhad, R. Yazdanni-rad, J. Alloys Compd. 491 (2010) 203–208.
[14] S. Cetinkaya, S. Eroglu, Int. J. Refract. Met. Hard Mater. 29 (2011) 214–220.
[15] J. Zhang, G. Zhang, S. Zhao, X. Song, J. Alloys Compd. 479 (2009) 427–431.
[16] D. Lou, J. Hellman, D. Luhulima, J. Liimatainen, Mater. Sci. Eng. A: Struct. 340 (2003) 155–162.
[17] H. Won, H. Nersisyan, C. Won, J. Nanopart. Res. 12 (2010) 493–500.
[18] M. Razavi, M.R. Rahimipour, A.H. Rajabi-Zamani, J. Alloys Compd. 436 (2007) 142–145.
[19] B. Cullity, S. Stock, Elements of X-ray Diffraction, Addison-Wesley, Reading, MA, 1978.
[20] D.R. Gaskell, Introduction to the Thermodynamics of Materials, 5th ed., Taylor & Francis, New York, 2008.
[21] C. Suryanarayana, Prog. Mater. Sci. 46 (2001) 1–184.
[22] D.A. Porter, K.E. Easterling, M.Y. Sherif, Phase Transformations in Metals and Alloys, 3rd ed., CRC Press, Boca Raton, FL, 2009.
[23] S.S.R. Tousi, R.Y. Rad, E. Salahi, I. Mobasherpour, M. Razavi, Powder Technol. 192 (2009) 346–351.